Sessile growth promotes PrrF- and 2-alkyl-4(1*H*)-quinolone-dependent iron regulation of the HSI-II type six secretion locus in *Pseudomonas aeruginosa*

Subject Area: Microbiology and Infectious Disease

Luke K. Brewer[1], Weiliang Huang[1], Brandy Hackert[1], Maureen A. Kane[1], Amanda G. Oglesby[1,2]*

University of Maryland, Baltimore, [1]School of Pharmacy, Department of Pharmaceutical Sciences and [2]School of Medicine, Department of Microbiology and Immunology, Baltimore, Maryland, 21201

*To whom correspondence should be addressed: aoglesby@rx.umaryland.edu

ABSTRACT

Pseudomonas aeruginosa is an opportunistic pathogen that is frequently associated with chronic, polymicrobial infections. *P. aeruginosa* possesses a complex regulatory network that modulates nutrient acquisition and virulence, but our knowledge of these networks is largely based on studies with shaking cultures, which are not likely representative of conditions during infection. Here, we provide proteomic, metabolic, and genetic evidence that regulation by iron, a critical metallo-nutrient, is altered in sessile *P. aeruginosa* cultures. We identified type VI secretion as a target of iron regulation in *P. aeruginosa* in static but not shaking conditions, and we demonstrate that this regulation occurs via PrrF sRNA-dependent production of 2-alkyl-4(1*H*)-quinolone metabolites. We further discovered that iron-regulated interactions between *P. aeruginosa* and a Gram-positive opportunistic pathogen, *Staphylococcus aureus*, are mediated by distinct factors in shaking versus sessile bacterial cultures. These results yield new bacterial iron regulation paradigms and highlight the need to re-define iron homeostasis in sessile microbial communities.

29 **INTRODUCTION**

30 Antimicrobial-resistant bacterial pathogens represent a substantial health risk, raising
31 concerns of a return to a "pre-antibiotic era." One prominent example is multi-drug resistant
32 (MDR) *Pseudomonas aeruginosa*, a Gram-negative opportunistic pathogen that is capable of
33 establishing acute infections of the blood and lung in immunocompromised individuals. *P.*
34 *aeruginosa* also causes chronic infections in surgical wounds, diabetic foot ulcers, and in the
35 lungs of individuals with cystic fibrosis (CF) and chronic obstructive pulmonary disease (COPD).
36 *P. aeruginosa* is the leading cause of morbidity among nosocomial pathogens, and is
37 responsible for over 10% of all hospital-acquired infections (1-7). Therapeutic options for *P.*
38 *aeruginosa* are rapidly dwindling due to the spread of antimicrobial resistance, underscoring the
39 need for novel antimicrobials that can be used to treat MDR infections. To that end, a more
40 complete understanding of the metabolic processes that contribute to *P. aeruginosa* survival
41 and pathogenesis during infection is necessary for the discovery and development of effective
42 therapeutics.

43 Iron is a required metallo-nutrient for most living organisms and has a significant impact
44 on the establishment and progression of *P. aeruginosa* infections (8, 9). During infection, the
45 host sequesters iron from invading pathogens through a process referred to as nutritional
46 immunity (10-12). In response to iron starvation, *P. aeruginosa* expresses several virulence
47 factors that cause host cell damage, presumably releasing iron and other nutrients from host
48 cells (13-17). Iron starvation also induces the expression of multiple systems that mediate high
49 affinity uptake of iron and heme (18, 19). Additionally, iron starvation induces expression of the
50 PrrF small regulatory RNAs (sRNAs), which post-transcriptionally reduce expression of non-
51 essential iron-dependent metabolic enzymes. The PrrF sRNAs are required for virulence in an
52 acute murine lung infection model and are also highly expressed in the lungs of CF patients (9,
53 20, 21). However, the specific mechanisms by which the PrrF sRNAs contribute to mammalian
54 infection remain unclear.

55 One prominent function of the PrrF sRNAs is their ability to indirectly promote the
56 production of several small secreted metabolites collectively referred to as 2-alkyl-4(1*H*)-
57 quinolones (AQs), which mediate a range of toxic activities against the host, as well as microbial
58 pathogens that co-colonize *P. aeruginosa*-infected hosts (20, 22-24). 2-alkyl-4-quinolone N-
59 oxides (AQNOs) are potent cytochrome inhibitors that obstruct respiratory metabolism in
60 mammalian and microbial cells (25-27). 2-alkyl-3-hydroxy-quinolone, which is more commonly
61 referred to as PQS, and 2-alkyl-4-hydroxyquinolones (AHQs) both function as quorum signaling
62 molecules and induce the expression of secreted factors that further inhibit growth of
63 mammalian and microbial cells (28-31). AQ synthesis is initiated by enzymes encoded by the
64 *pqsABCDE* operon, with PqsA catalyzing the first step with the conversion of anthranilate into
65 anthraniloyl-CoA (32). The PrrF sRNAs promote AQ production by repressing the translation of
66 the anthranilate degradation enzyme complexes AntABC and CatBCA (16), which degrade
67 anthranilate to metabolites that enter the tricarboxylic acid (TCA) cycle. Thus, the PrrF sRNAs
68 spare anthranilate for AQ production and are therefore required for optimal AQ production in
69 iron-depleted conditions (9, 20, 23, 33) .
70 In accordance with PrrF promoting AQ production in iron-depleted environments, we
71 previously discovered that iron starvation enhances AQ-dependent antimicrobial activity against
72 the Gram-positive pathogen *Staphylococcus aureus*, which can co-colonize with *P. aeruginosa*
73 in chronic wounds and in CF lung infections (20, 23). Surprisingly, these previous studies
74 showed that the *prrF* locus was not required for iron-regulated antimicrobial activity, and several
75 possible explanations for this have been considered. One explanation that has not been
76 investigated is that earlier studies used either agar plates or static liquid cultures, which are
77 likely distinct from the shaking liquid cultures historically used to study iron regulation. While
78 aerobic shaking cultures are exposed to constant aeration and perturbation to promote
79 homogenous cultures, *P. aeruginosa* infections are typically more heterogeneous and feature
80 planktonic as well as adherent biofilm communities of *P. aeruginosa*, particularly during chronic

81 infections. Changes in the iron metabolism and iron regulatory factors in response to aeration
82 and perturbation have been documented in other bacterial species, suggesting a regulatory link
83 between iron regulated metabolism and sessile growth that may be common among other
84 bacterial species (34, 35). Because of the broad impact of iron on *P. aeruginosa* physiology, we
85 hypothesized that sessile growth would likewise alter iron-regulated metabolism in *P.*
86 *aeruginosa*, potentially revealing novel iron regulatory pathways that are more relevant during
87 infection.

88 In the current study, we sought to identify targets of iron and PrrF regulation during
89 sessile growth of *P. aeruginosa* using an untargeted proteomics-based approach. Our results
90 revealed a number of proteins that were differently affected by iron and PrrF in sessile versus
91 shaking cultures. Amongst these were the proteins for phenazine biosynthesis, which were
92 repressed by iron in sessile conditions, while recent studies show they are induced by iron in
93 shaking conditions (12, 36). We also discovered PrrF positively affects the expression of the
94 Hcp1 secretion island II type VI secretion system (HSI-II T6SS) in *P. aeruginosa*, and that this
95 regulation is due to PrrF-mediated AQ production. Moreover, while PrrF is not required for
96 antimicrobial activity against *S. aureus* in sessile conditions, we found that it still promotes the
97 production of AQs in sessile conditions. However, the relative abundances and roles of
98 individual AQ species for interspecies interactions varied between shaking versus sessile
99 cultures, thereby altering the requirement of PrrF for antimicrobial activity. Lastly, we show that
100 reduced oxygen availability in sessile cultures is not solely responsible for the changes in iron
101 regulation observed in this study. Combined, these results indicate that sessile bacterial
102 communities use unique regulatory and metabolic networks to adapt to decreased nutrient
103 availability, likely affecting the production of key virulence determinants.
104
105

106 **MATERIALS AND METHODS**

107 **Bacterial strains and growth conditions.** Bacterial strains used in this study are listed
108 in **Supplementary Table S1**. Lysogeny broth (LB) and agar (LA) were prepared using 10g/L
109 NaCl (Sigma, St Louis, MO), 10g/L tryptone, and 5g/L yeast extract, 15g/L agar when applicable
110 (Becton-Dickinson, Franklin Lakes, NJ). *P. aeruginosa* and *S. aureus* strains were both routinely
111 grown on LA from freezer stock. Five isolated colonies of each strain were selected from
112 overnight-incubated agar plates and inoculated into 5mL LB. For iron starvation studies,
113 bacterial strains were grown in a Chelex-treated and dialyzed trypticase soy broth (DTSB)
114 prepared as previously described (16). Media dialysis was carried out using Spectra/Por®2
115 dialysis membrane tubing (29mm diameter) with a molecular weight cutoff of 12-14kD
116 (Repligen, Waltham, Ma).

117 For co-culture assays, quantitative real time PCR (qRT-PCR) analysis, and mass
118 spectrometry-assisted metabolite and proteome studies, *S. aureus* and *P. aeruginosa* cultures
119 were diluted into 1.5mL of DTSB with or without 100μM (high iron) $FeCl_3$ supplementation, to an
120 absorbance (OD_{600}) of 0.08 and 0.05, respectively. Mono- and co-cultures of *P. aeruginosa* and
121 *S. aureus* were prepared in DTSB media and incubated at 37˚C for 18 hours in a shaking
122 incubator. Shaking aerobic cultures were incubated in 1.5mL of DTSB media in 14mL round
123 bottom tubes and closed with a foam stopper to allow for sufficient aeration. Sessile cultures
124 were incubated in 1.8mL DTSB media in 6-well polystyrene culture plates, which were covered
125 in breathe-easy wrap to prevent evaporation. During incubation, cultures were grown at a
126 shaking rate of either 250rpm (shaking conditions) or 0rpm (static conditions). Microaerobic co-
127 cultures were grown in identical growth conditions as shaking cultures, except culture tubes
128 were placed into an air-tight candle jar in the presence of a CampyPak (BD Diagnostics, NJ,
129 USA). Sealed candle jars were secured in a shaking incubator and incubated for 18 hours at
130 37˚C and a shaking rate of 250rpm.

131

132 **Quantitative label-free proteomics.** Cell cultures were prepared for proteomics
133 analysis as described previously (36). Briefly, cells were harvested by centrifugation and
134 washed in phosphate-buffered saline prior to lysis in 4% sodium deoxycholate. Lysates were
135 washed, reduced, alkylated and trypsinolyzed on filter (37, 38). Tryptic peptides were separated
136 using a nanoACQUITY UPLC analytical column (BEH130 C18, 1.7 µm, 75 µm x 200 mm,
137 Waters) over a 165-minute linear acetonitrile gradient (3 – 40%) with 0.1 % formic acid on a
138 Waters nano-ACQUITY UPLC system and analyzed on a coupled Thermo Scientific Orbitrap
139 Fusion Lumos Tribrid mass spectrometer. Full scans were acquired at a resolution of 120,000,
140 and precursors were selected for fragmentation by higher-energy collisional dissociation
141 (normalized collision energy at 32 %) for a maximum 3-second cycle. Tandem mass spectra
142 were searched against *Pseudomonas* genome database PAO1 reference protein sequences
143 (39) using Sequest HT algorithm and MS Amanda algorithm with a maximum precursor mass
144 error tolerance of 10 ppm (40, 41). Carbamidomethylation of cysteine and deamidation of
145 asparagine and glutamine were treated as static and dynamic modifications, respectively.
146 Resulting hits were validated at a maximum false discovery rate of 0.01 using a semi-
147 supervised machine learning algorithm Percolator (42). Label-free quantifications were
148 performed using Minora, an aligned AMRT (Accurate Mass and Retention Time) cluster
149 quantification algorithm (Thermo Scientific, 2017). Protein abundance ratios between the high
150 iron cultures and the low iron cultures were measured by comparing the MS1 peak volumes of
151 peptide ions, whose identities were confirmed by MS2 sequencing as described above. Gene
152 function and pathway analysis was completed using information from the *Pseudomonas*
153 genome database (39), KEGG database (43), *Pseudomonas* metabolome database (44), and
154 the STRING database (45).
155
156 **Real time PCR analysis.** Quantitative real time PCR (qRT-PCR) analysis was
157 conducted on at least three biological replicates of the PAO1 reference strain, the isogenic

158 Δ*prrF* mutant, or Δ*pqsA* mutant grown in DTSB supplemented with either 100μM or 0μM iron. *P.*
159 *aeruginosa* cells were lysed after 18 hours using 2.5mg/mL lysozyme and incubated at 37˚C for
160 30 minutes. RNA extraction was performed using the RNeasy mini kit (QIAGEN, Germantown,
161 MD). Real-time qualitative PCR analysis was performed as described previously (9) using an
162 Applied Sciences StepOne Plus Real Time PCR System (Life Technologies, Carlsbad, CA).
163 Primer and probe sequences used for gene expression analysis are listed in **Supplementary**
164 **Table S2**. Quantitation of cDNA was carried out using standard curves compiled for individual
165 gene targets. *P. aeruginosa* expression data was normalized to *oprF* expression in aerobic
166 shaking conditions, or *omlA* in either microaerobic shaking conditions or sessile growth
167 conditions.
168
169 **Quantitation of AQs using liquid chromatography-tandem mass spectrometry.** AQ
170 quantitation was carried out as previously reported (46). Briefly, 300μL of culture were
171 harvested and spiked with a 25μM stock nalidixic acid internal standard to a final concentration
172 of 500nM, followed by an extraction using ethyl acetate with 0.1% acetic acid. The organic
173 phase containing extracted AQs was harvested from each sample, dried down, and
174 resuspended in 300μL of 0.1% formic acid suspended in 1:1:1 (v/v/v) mixture of methanol,
175 water, and acetonitrile. Extracts were analyzed via quantitative liquid chromatography-tandem
176 mass spectrometry (LC-MS/MS) using multiple reaction monitoring (MRM) performed on a
177 Waters ACQUITY UHPLC coupled to a Xevo TQ-XS tandem quadrupole mass spectrometer in
178 positive ion mode**.**
179 In order to quantify the amount of PQS and AHQ export from sessile and shaking
180 cultures, supernatants were analyzed in 5 biological replicates of wild type PAO1 using LC-
181 MS/MS and compared to whole culture extracts. 300μL of 18h DTSB cell cultures were either
182 subjected to ethyl acetate extraction or were centrifuged for 5 minutes at 21000rcf, and cell
183 supernatants were transferred to fresh eppendorf tubes. Cell supernatants were then subjected

184 to AQ extraction using ethyl acetate with 0.1% acetic acid prior to LC-MS/MS analysis, as
185 described above.
186
187 **AQ complementation.** For chemical complementation of the Δ*pqsA* mutant, individual
188 AQ standards were obtained commercially from the following sources: 2-heptyl-3-hydroxy-4-
189 (1*H*)-quinolone (C7-PQS) and 2-heptyl-4-quinolone (HHQ) were both purchased from Millipore
190 Sigma (Burlington, MA, USA); 2-nonyl-3-hydroxy-4-(1*H*)-quinolone (C9-PQS) was obtained from
191 Cayman Chemical Company (Ann Arbor, MI, USA); 2-nonyl-4-quinolone (NHQ) was purchased
192 from Combi-Blocks (San Diego, CA, USA). 50μM stock solutions of each AQ were then
193 prepared by suspending dried samples in methanol, incubating at 37˚C for 10 minutes, and then
194 sonicating samples in a sonicating water bath for 20 seconds. Cell cultures were prepared by
195 incubating wild type PAO1 and Δ*pqsA* strains in low or high iron DTSB at a shaking rate of
196 250rpm (shaking conditions) or 0rpm (sessile) at 37˚C, as described above. After 18h
197 incubation, 400μL of cell culture were removed and diluted in RNAlater (Invitrogen, Carlsbad,
198 CA) for qRT-PCR analysis as described above. An additional 50μL of culture was removed and
199 subjected to ethyl acetate extraction for targeted LC-MS/MS analysis. Chemically
200 complemented Δ*pqsA* groups were supplemented with either a mixture of C7-PQS and C9-PQS
201 to a final concentration of 15μM and 8μM, respectively, or a mixture of HHQ and NHQ to a final
202 AQ concentration of 3 μM and 4μM, respectively. Wild type and Δ*pqsA* control cultures were
203 treated with an equivalent volume of MeOH to account for MeOH-mediated effects on T6SS
204 gene expression. Complemented and un-complemented strains were then incubated for 2 hours
205 under identical incubation parameters as described above. After 2 hours, 400μL of culture were
206 diluted in RNAlater for qRT-PCR analysis, while an additional 50μL of culture were subjected to
207 ethyl acetate extraction for targeted LC-MS/MS analysis.
208 For complementation of the Δ*pqsA* mutant with culture supernatants, PAO1 donor
209 cultures were grown in 1.5mL of either low or high iron supplemented DTSB at 37˚C, and

210 incubated at a shaking rate of either 250rpm or 0rpm, as described above. After 18 hours, donor
211 cultures were centrifuged at 20,000rcf for 4 minutes and supernatants were subsequently
212 removed and filter sterilized using 28mm, 0.20μM syringe filters (Corning Inc., NY, USA). 50μL
213 of filtered supernatants were removed and subjected to ethyl acetate to confirm the presence of
214 AQs via LC-MS/MS. Acceptor cultures were incubated under identical conditions as those
215 described for donor cultures. After 18 hours incubation, 400μL of acceptor cultures were
216 removed and diluted into 400μL of RNAlater for qRT-PCR analysis, while an additional 50μL
217 was removed and subjected to ethyl acetate extraction for LC-MS/MS analysis. 700μL of
218 remaining culture were then transferred to microcentrifuge tubes and centrifuged at 20,000rcf
219 for 4 minutes. Upon centrifugation, wild type and Δ*pqsA* strains were either pipette mixed back
220 into solution, serving as positive and negative controls, respectively, or their cell supernatants
221 were removed and replaced with supernatants from donor cultures grown under identical
222 conditions. Once resuspended, cultures were transferred into fresh 15mL culture tubes and
223 incubated for 2 hours under their previous incubation parameters. After 2 hours, 400μL of
224 acceptor culture were diluted into 400μL of RNAlater for qRT-PCR analysis, and an additional
225 50μL were removed and subjected to ethyl acetate extraction for subsequent LC-MS/MS
226 analysis.
227
228 **Co-culture studies.** 400μL of *P. aeruginosa* and *S. aureus* mono- and co-cultures were
229 harvested at 15000rcf for 5 minutes. Cell pellets were resuspended in 400μL of 0.1% Triton-X in
230 phosphate-buffered saline (PBS) and vortexed rigorously. From these resuspensions, serial
231 dilutions were prepared in 0.1% Triton-X in PBS. 10μL of each dilution was spotted onto Baird-
232 Parker agar plates and Pseudomonas Isolation Agar (PIA) plates to select for *S. aureus* and *P.*
233 *aeruginosa* growth, respectively. Upon spotting 10μL of dilutions onto agar plates, the plates
234 were tilted to facilitate even drips across the plate surface. PIA plates were incubated at 37˚C
235 for 18 hours and colony forming units (CFU) were counted. Baird-Parker plates were incubated

236 for 37˚C for 48 hours to allow for adequate growth of *S. aureus* small-colony variants observed
237 in some assays prior to counting CFUs.
238
239 **Statistics**. Statistically significant changes in cell viability, RNA gene expression, and
240 AQ concentrations between treatment groups were identified using a two-tailed students t-test
241 on Microsoft Excel 2013, with a significance threshold of p value ≤ 0.05. Protein expressions
242 that changed 2-fold or more with an FDR adjusted p-value < 0.05 were considered statistically
243 significant.
244
245 **RESULTS**
246 **Proteomics reveals altered iron-regulation in sessile *P. aeruginosa* cultures.** Our
247 current knowledge of *P. aeruginosa* iron regulation is largely restricted to shaking cultures (14,
248 16, 19, 23, 36, 47). To determine whether global iron regulatory pathways are altered in sessile
249 cultures *of P. aeruginosa*, we applied a label-free, LC-MS/MS-based proteomics methodology
250 recently described by our laboratories (36). Using this unbiased approach, we determined the
251 proteomes of static and shaking cultures of PAO1 and the isogenic Δ*prrF* mutant grown in
252 chelexed and dialyzed TSB medium (DTSB), supplemented with or without 100μM $FeCl_3$. Mass
253 spectra were identified using a PAO1 reference proteome, which were in turn validated to a
254 false discovery rate of 0.01 to ensure proper assignment of protein identities.
255 Initially, we sought to confirm whether iron regulatory effects previously identified in
256 shaking conditions were similar to shaking cultures analyzed in the current study. For this, we
257 identified proteins whose levels showed a statistically significant (FDR adjusted *p*-value <0.05)
258 log fold change (LFC) > 1 upon iron starvation. This analysis revealed 178 and 191 proteins that
259 were significantly induced and repressed, respectively, by iron starvation (**Supplementary**
260 **Dataset S1**). As previously observed (14, 19, 48-52), iron starvation significantly increased
261 proteins for the siderophore (pyoverdine and pyochelin) and heme uptake systems, as well as

262 several iron-regulated virulence factors, during shaking growth (**Fig. 1A**). Also as previously
263 observed, iron-containing proteins involved in the TCA cycle and oxidative metabolism,
264 including aconitase A, succinate dehydrogenase B, and catalase, were induced by iron in a
265 PrrF-dependent manner under shaking conditions (**Fig. 1B**) (16, 53). We also observed PrrF-
266 dependent iron regulation of more recently identified PrrF targets in shaking conditions,
267 including proteins involved in Fe-Sulfur cluster biogenesis (IscS, IscU) and amino acid
268 metabolism (IlvD) (**Fig. 1B**) (36). Contrary to previous real-time PCR and microarray analyses
269 showing iron induction of the *antABC* mRNAs (36), neither iron supplementation nor *prrF*
270 deletion significantly affected levels of the AntABC proteins for anthranilate degradation under
271 shaking conditions (**Fig. 1B**). Overall however, this analysis replicated many of the global iron
272 regulatory pathways observed in previous studies.

273 We next determined whether known targets of PrrF and iron regulation under shaking
274 conditions were similarly regulated under sessile conditions. Iron repression of siderophore and
275 heme uptake proteins was largely retained during static growth, indicating that these iron
276 regulatory pathways are not altered under sessile conditions (**Fig. 1A**). In contrast, iron and PrrF
277 regulation of several proteins involved in the TCA cycle or oxidative stress protection was
278 reduced or eliminated in static conditions (**Fig. 1B**). We also noted robust iron induction of the
279 anthranilate degradation proteins AntABC and CatBCA, which occurred in a PrrF-independent
280 manner (**Fig. 1B**)**,** in agreement with trends we observed in subsequent qRT-PCR analysis of
281 *antR* and *antA* under identical growth conditions **(Supplementary Fig. S1)**. Combined, these
282 data indicate that PrrF-dependent iron regulatory pathways are altered in static conditions.

283 To determine if there are iron or PrrF regulatory effects that are unique to either sessile
284 or shaking growth, we mined our proteomics dataset for proteins whose levels were altered by
285 iron depletion in either sessile or shaking conditions, but not in both, by an LFC ≥ 1 and an FDR
286 adjusted *p* value ≤ 0.05. Approximately 410 proteins demonstrated significantly altered iron
287 regulation in response to growth conditions. Of these, 126 of these were specifically iron

288 induced and 93 were iron repressed in shaking but not static conditions, while 78 were iron
289 induced and 129 were iron repressed only in static conditions (**Supplementary Tables S3-S7**
290 **and Dataset S1**). Approximately 50% of the proteins affected by iron supplementation in static
291 conditions were unaffected by iron in the Δ*prrF* mutant (**Supplementary Tables S3-S7 and**
292 **Dataset S1**), indicating PrrF still mediates iron homeostasis during these growth conditions,
293 despite the loss of PrrF-mediated iron regulation on previously identified targets as shown in
294 **Fig. 1B**.
295 STRING network analysis was next used to identify relationships between the proteins
296 within each of these four groups. Several of the proteins that were induced by iron in shaking
297 conditions but not in static conditions were related to motility, including proteins for flagellar
298 assembly (FlgA, FlgL, FliC, and FliI), a chemotaxis-associated protein (ChpA), and proteins
299 involved in twitching pilus formation (PilV, PilY2, and FimU) **(Supplementary Dataset S1).**
300 Proteins that were significantly induced by iron depletion in static but not shaking cultures
301 included numerous enzymes required for synthesis of the redox cycling phenazine metabolites
302 and the pyochelin siderophore, as well as proteins encoded by the HSI-II T6SS locus (**Fig. 2A,**
303 **Supplementary Tables S4-S5)**. Iron regulation of the phenazine and pyochelin synthesis
304 proteins occurred in a PrrF-independent manner, while iron regulation of many of the T6SS
305 proteins was either reduced or lost in the Δ*prrF* mutant (**Fig. 2B**). Moreover, we found that *prrF*
306 deletion had a negative effect on T6SS proteins in static but not shaking conditions
307 **(Supplementary Dataset S1**). The identification of T6SS as iron- and PrrF-regulated during
308 static but not shaking conditions was particularly intriguing, as this contact-dependent secretion
309 system is known to mediate virulence and interbacterial interactions that may be more relevant
310 in static conditions than in highly perturbed, shaking conditions. No complementarity was
311 identified between the PrrF sRNAs and the mRNAs encoding these proteins, thus we
312 hypothesized expression of these proteins is indirectly regulated by PrrF.
313

314 **HSI-II T6SS genes are differentially regulated by AQs in shaking versus static**
315 **conditions.** No previous reports have demonstrated a regulatory link between the PrrF sRNAs
316 and T6SS, nor were we able to identify complementarity between PrrF and T6SS secretion
317 mRNA sequences. Previous reports, however, have demonstrated that PrrF sRNAs are
318 necessary for full AQ production via repression of the anthranilate-degrading enzymes (9, 33).
319 AQs, in turn, induce expression of several virulence-associated genes, including genes involved
320 in T6SS (54, 55). We therefore first sought to determine whether defects in T6SS gene
321 expression observed in the Δ*prrF* mutant during our proteomics analysis were due to a partial
322 loss of AQ production. To test this, we performed targeted expression analysis of T6SS genes
323 in our wild type, Δ*prrF,* and Δ*pqsA* strains grown in sessile conditions using quantitative real
324 time PCR (qRT-PCR). Specifically, we analyzed the expression of genes encoding proteins that
325 demonstrated PrrF dependence in our proteomics analysis, including *clpV2*, *fha2*, and *lip2*. In
326 agreement with our proteomics analysis, the Δ*prrF* mutant exhibited statistically significant
327 decreases in expression of each of these genes when grown in static conditions (**Fig. 3A**).
328 Moreover, the Δ*pqsA* mutant demonstrated even more dramatic decreases in the expression of
329 *clpV2, fha2,* and *lip2* relative to wild type PAO1 (**Fig. 3A**), supporting the notion that AQs are
330 necessary for the expression of T6SS genes in sessile cultures. In contrast, neither *prrF* nor
331 *pqsA* were required for T6SS gene expression in shaking conditions (**Fig. 3B**), supporting the
332 hypothesis that AQ regulation of T6SS is enhanced by sessile growth. Furthermore, we
333 observed that iron regulation of T6SS genes was either reduced or eliminated in shaking
334 conditions (**Fig. 3B)**. Thus, iron regulation of T6SS in strain PAO1 occurs in a PrrF- and AQ-
335 dependent manner, and at least under the current media conditions, is restricted to sessile
336 growth.
337
338 **AHQ concentrations are increased in static growth conditions.** Our proteomics and
339 qRT-PCR analysis indicated that AQ regulation of T6SS genes is specific to sessile conditions,

340 although the underlying mechanism of this shift was not clear. Previous reports have
341 demonstrated that static growth can dramatically impact broad aspects of *P. aeruginosa*
342 physiology, including expression of virulence traits. These reports have suggested that
343 diminished oxygen availability in static conditions plays a defining role in mediating these effects
344 (56-58). Additional studies showed that oxygen limitation decreases PQS production while
345 increasing production of the PQS precursor molecules, AHQs (59). As such, we hypothesized
346 that oxygen limitation resulting from sessile growth conditions would favor production of AHQs,
347 potentially influencing AQ regulation of T6SS.
348 To test this, we used a validated LC-MS/MS method (46) to measure levels of various
349 AQ species in shaking and sessile cultures of wild-type PAO1 and the isogenic Δ*prrF* mutant.
350 As previously observed (23, 33), PrrF was required for optimal production of the C7 and C9
351 congeners of PQS, AQNO, and AHQ in shaking conditions (**Fig. 4A,B,C, white bars**). Similarly,
352 PrrF was required for optimal production of each AQ congener in static cultures (**Fig. 4A,B,C,**
353 **gray bars**), indicating that PrrF still promotes AQ production in sessile growth conditions. We
354 also observed a dramatic decrease in the levels of the C7 and C9 congeners of both PQS and
355 AQNO in sessile cultures (**Fig. 4 A,B, gray bars**), likely due to the previously reported oxygen
356 requirement for activity of the PqsH and PqsL enzymes (59, 60). The decrease in PQS in static
357 cultures corresponded to an increase in the AHQ congeners, both in the wild type and Δ*prrF*
358 strains (**Fig. 4C, gray bars versus white bars**). However, when we performed analysis of
359 cultures grown in shaking microaerobic conditions, AHQ levels were not significantly enhanced
360 relative to shaking aerobic cultures, despite decreased production of PQS and AQNO
361 congeners (**Fig. 4A,B,C striped bars versus white bars**). This indicates that increased AHQ
362 levels in sessile cultures are not solely due to reduced oxygen availability, but that sessile
363 growth causes distinct changes in *P. aeruginosa* AQ metabolite profiles.
364

365 **Wild type supernatants partially restore T6SS expression in static Δ*pqsA* cultures.**
366 Since AQ-dependent induction of T6SS corresponded closely with increases in the production
367 of AHQ quorum signaling molecules, we speculated that AHQs might possess enhanced
368 regulatory activity over T6SS gene expression. To test this hypothesis, we incubated the wild
369 type and Δ*pqsA* strains in DTSB under shaking or static conditions. After 18h incubation, we
370 supplemented the Δ*pqsA* mutant culture with a mixture of synthesized C7 and C9 congeners of
371 either PQS or AHQ, each at concentrations equivalent to those observed in iron-depleted PAO1
372 cultures **(Fig. 4A,C, white and gray bars),** and we grew these cultures for an additional 2
373 hours. We measured expression of T6SS systems genes in these cultures before AQ
374 supplementation (18h of growth) and two hours after supplementation (20h total growth). These
375 again data confirmed that *pqsA* is required for numerous HSI-II T6SS genes in static condition
376 but not shaking conditions (**Fig. S2)**. Surprisingly, the AHQ and PQS mixtures both significantly
377 induced T6SS gene expression in shaking cultures of the Δ*pqsA* mutant, but not in sessile
378 cultures **(Fig. S2**)**.** The un-supplemented wild type and Δ*pqsA* controls did not demonstrate
379 statistically significant induction over the 2-hour incubation period, with or without shaking (**Fig.**
380 **S2**), verifying that the induction of T6SS expression in supplemented shaking cultures was not
381 due to longer growth. LC-MS/MS analysis of supplemented cultures before and after the 2-hour
382 incubation period indicated that AHQ is converted to PQS in shaking cultures, and to a lesser
383 extent in static cultures (**Fig. S3)**. As a result, it was unclear if the observed induction in T6SS
384 genes during shaking conditions was caused by AHQs or PQS.
385 We next wondered if the lack of induction of T6SS expression by AQs in static conditions
386 above was due to differences in exogenous versus endogenous AQ delivery. PQS is known to
387 promote the formation of and insert into *P. aeruginosa* outer membrane vesicles (OMVs), which
388 mediate transport of PQS and other metabolites from cell to cell. Thus, it was possible that
389 exogenous delivery of MeOH-solubilized AQs did not accurately model the biology that
390 surrounds quinolone-mediated quorum sensing in sessile and shaking cultures. LC-MS/MS

391 analysis of supernatants and whole cultures from wild type *P. aeruginosa* demonstrated that
392 sessile cultures exhibited a higher proportion of C7- and C9-PQS outside the cell (**Fig. S4**),
393 further indicating that distinct trends in AQ-mediated QS may exist in sessile cultures versus
394 shaking conditions. To examine this possibility in light of T6SS expression, we supplemented
395 the Δ*pqsA* mutant with sterile filtered supernatants from wild type PAO1 cultures, thus
396 conserving potential delivery and transport mechanisms that exist in wild type cultures.
397 Specifically, we grew wild type and Δ*pqsA* strains for 18 hours in iron-deplete DTSB under
398 shaking or static conditions and then centrifuged the cultures and removed the supernatant. We
399 then resuspended these cultures in the sterile filtered supernatants from wild type PAO1 grown
400 under identical conditions, effectively supplementing these strains with AQs in their most
401 biologically relevant state. Supplemented cultures and un-supplemented control cultures were
402 incubated for an additional two hours with the transplanted medium. At 18h, we observed the
403 characteristic requirement of *pqsA* for T6SS gene expression in sessile but not shaking cultures
404 (**Fig. S5**). Notably, incubation with wild type PAO1 supernatants resulted in a significant
405 induction of all measured HSI-II T6SS genes in the Δ*pqsA* mutant grown under static conditions
406 but not in shaking conditions, indicating a differential impact of AQs on T6SS gene expression in
407 response to perturbation (**Fig. 5**). Thus, delivery of AQs and/or AQ-induced exoproducts in their
408 natively produced state allows for induction of T6SS expression in static but not shaking DTSB
409 cultures.
410
411 **PrrF-mediated antimicrobial activity is altered by sessile growth conditions.** We
412 next probed the impact of sessile growth on iron-regulated interactions with *S. aureus*. As
413 discussed above, we previously discovered that iron starvation enhances AQ-dependent
414 antimicrobial activity against *S. aureus* on agar plates as well as in a transwell co-culture system
415 (20, 23). Surprisingly, the Δ*prrF* mutant demonstrated similar antimicrobial activity to wild type
416 PAO1 in this previous study, suggesting that PrrF's effects on AQs may be distinct in these

417 assays (23). In light of our proteomic, qPCR, and metabolite analysis discussed above, we
418 hypothesized that the sessile nature of these co-culture systems may influence relative levels of
419 AQs that are produced, thus altering the impact of PrrF on antimicrobial activity.

420 To test this idea, we co-inoculated mono- and co-cultures of *P. aeruginosa* strain PAO1
421 and *S. aureus* strain USA300 in DTSB, supplemented with or without 100μM $FeCl_3$, and grew
422 them either statically or in a shaking incubator at 250rpm. After 18 hours, viability of *P.*
423 *aeruginosa* and *S. aureus* was quantified by enumerating CFUs on selective PIA and Baird
424 Parker agar, respectively. In agreement with earlier studies showing that AQs mediate
425 antimicrobial activity against *S. aureus*, USA300 viability was reduced significantly during low
426 iron co-culture with PAO1 static conditions, whereas the Δ*pqsA* mutant did not exhibit
427 antimicrobial activity against USA300 (**Fig. 6B, white bars**). Also in agreement with our earlier
428 work, iron limitation significantly enhanced antimicrobial activity of PAO1 against USA300 in
429 sessile co-cultures (**Fig. 6B, white versus gray bars**). We observed similar AQ-dependent,
430 iron-regulated antimicrobial activity in shaking cultures, though *S. aureus* viability was reduced
431 approximately 50,000-fold in low iron co-cultures with PAO1, signifying more robust killing than
432 in sessile co-cultures (**Fig. 6A, white bars).** Notably, the Δ*prrF* mutant was defective for
433 antimicrobial activity relative to the isogenic parent strain PAO1 in low iron shaking co-cultures
434 (**Fig. 6A, white bars**), a result that contrasted with our previous and current reports on sessile
435 co-cultures (23). *P. aeruginosa* viability was not affected by iron supplementation or deletion of
436 either *pqsA* or *prrF* in any of the conditions tested (**Fig. 6**), verifying that changes in
437 antimicrobial activity were not the result of changes in the viability of the *P. aeruginosa* Δ*pqsA* or
438 Δ*prrF* mutants.

439 These results indicated that the influence of PrrF on antimicrobial activity is reduced
440 during sessile growth, which was surprising since PrrF is still required for optimal AQ production
441 during sessile growth (**Fig. 4, white and gray bars)**. However, our LC-MS/MS analysis also
442 showed that AHQs were much more abundant in static cultures compared to shaking cultures of

443 both the wild type and Δ*prrF* mutant (**Fig. 4C, gray bars**). Thus, AHQ production by the Δ*prrF*
444 mutant in sessile culture, even if it is reduced compared to wild type, may still be robust enough
445 to promote antimicrobial activity against *S. aureus*. Conversely, our LC-MS/MS analysis showed
446 that shaking microaerobic cultures did not allow for a similar increase in AHQ levels (**Fig. 4C,**
447 **striped bars**). To investigate whether the ability of the Δ*prrF* mutant to maintain antimicrobial
448 activity in sessile growth was due solely to oxygen limitation or due to the increase in AHQs, we
449 co-cultured *S. aureus* with *P. aeruginosa* wild type PAO1, Δ*pqsA,* or Δ*prrF* strains with shaking
450 in either microaerobic or aerobic conditions. Similar to what was observed in shaking aerobic
451 cultures, the Δ*prrF* mutant was defective for antimicrobial activity in shaking microaerobic
452 conditions (**Fig. 7A,B**), indicating that changes in PrrF-dependent antimicrobial activity during
453 sessile growth are not solely due to changes in oxygen availability, but may instead correlate
454 with an overall increase in AHQ levels.
455
456 **Phenazines and pyochelin are not solely required for antimicrobial activity in**
457 **sessile co-culture.** Since iron-regulated antimicrobial activity occurs in a PrrF-independent
458 manner in sessile cultures, we sought to determine the impact of iron regulated, PrrF-
459 independent pathways on antimicrobial activity in static conditions. To do so, we focused on the
460 impact of phenazine and pyochelin biosynthesis proteins, which were induced by iron starvation
461 in a PrrF-independent manner in our proteomics dataset (**Fig. 2**). To determine the impact of
462 these systems on antimicrobial activity, we used agar co-cultures of *S. aureus* with a phenazine-
463 deficient PA14 Δ*phzA1-A2* mutant and its isogenic PA14 parent strain, as well as a pyochelin-
464 deficient PAO1 Δ*pchEF* mutant and its PAO1 parent strain. The *S. aureus* strain USA300 was
465 swabbed onto agar plates containing low or high iron DTSB media, and wild-type *P. aeruginosa*
466 strains or their isogenic mutant strains were spotted onto the monolayers. Both the phenazine-
467 deficient Δ*phz* mutant and pyochelin-deficient Δ*pchEF* mutants demonstrated wild type levels of
468 antimicrobial activity against *S. aureus* (**Fig. S6**), suggesting that neither phenazines nor

469 pyochelin alone account for enhanced antimicrobial activity in static, low iron conditions. A
470 siderophore deficient double mutant carrying deletions of *pchEF* and the pyoverdine synthesis
471 gene *pvdA* in a PAO1 background was completely defective for antimicrobial activity in these
472 conditions (**Fig. S6**). Single deletion of the *pvdA* gene did not eliminate antimicrobial activity
473 (**Fig. S6**), suggesting that the composite effect of these two siderophores is critical in static
474 conditions.

475 Because sessile growth also triggered iron regulation of HSI-II T6SS genes, albeit in a
476 PrrF-dependent fashion, we tested the impact of this T6SS locus on antimicrobial activity using
477 a Δ*clpV2* transposon insertion mutant, which is expected to be defective for HSI-II T6SS
478 function, from the University of Washington PAO1 Transposon Library (61). The Δ*clpV2*
479 transposon mutants showed reduced antimicrobial activity against *S. aureus* when compared to
480 our laboratory's PAO1 strain (**Fig. S6, S7**). However, the parental mPAO1 strain used for
481 generating the transposon library exhibited very low baseline antimicrobial activity on agar
482 plates (**Fig. S6**) or in liquid shaking or static cultures (**Fig. S7A,B**), making it difficult to interpret
483 the impact of *clpV2* on this process. Thus further studies will be necessary to determine the
484 relative impact of HSI-II T6SS against *S. aureus*.

485

486 **Sessile growth alters the impact of specific AQs on antimicrobial activity.** We next
487 questioned whether individual AQ species differentially impacted antimicrobial activity in shaking
488 versus static cultures. AQNOs are known to induce fermentative metabolism in *S. aureus,* and
489 subsequently the formation of slow-growing small colony variants of *S. aureus;* PQS- and AHQ-
490 mediated quorum sensing mediates production of virulence factors such as rhamnolipids,
491 phenazines, and hydrogen cyanide (30, 62, 63). To test the relative contributions of these AQ
492 species, we co-incubated *S. aureus* with either a PQS-deficient mPAO1 Δ*pqsH* transposon
493 insertion mutant or an AQNO-deficient PAO1 Δ*pqsL* strain in liquid co-cultures. Similar to
494 previous analysis reported by our lab and others (20, 24), *pqsH* was not required for

495 antimicrobial activity in either shaking or static conditions (**Fig. S8A,B**). In contrast, Δ*pqsL* was
496 completely defective for antimicrobial activity against *S. aureus* in shaking cultures but retained
497 some antimicrobial activity in sessile co-cultures (**Fig. 8A,B**). While antimicrobial activity of the
498 Δ*pqsL* mutant is less robust than the wild type parent, these data suggest that the role of
499 AQNOs in antimicrobial activity is reduced in sessile co-cultures, supported by the significant
500 decrease in AQNO production observed in the wild type and Δ*prrF* strains in sessile cultures
501 (**Fig. 4**). Combined, these results demonstrate that different classes of AQ metabolites have
502 distinct impacts on polymicrobial interactions in sessile versus shaking cultures.
503

504 **DISCUSSION**

505 The PrrF sRNAs are critical for *P. aeruginosa* pathogenesis due to their ability to
506 mediate numerous biological functions upon iron starvation (9). Amongst these is the Δ*prrF*
507 mutant's well-documented defect in the production of AQs (23, 33), which are necessary for
508 virulence in several infection models (64-66). In the current study, we identified the HSI-II T6SS
509 loci as a novel PrrF-responsive system, and we provide evidence that this iron regulatory effect
510 is promoted by sessile growth and mediated by quorum signaling AQs. The T6SS contributes to
511 *P. aeruginosa* virulence in several models of infection (54, 55) and also facilitates inter-bacterial
512 interactions in *P. aeruginosa* and other bacterial species (67, 68). T6SS mediates cell-to-cell
513 interactions that are contact dependent and likely disrupted in shaking cultures (67), making this
514 newly elucidated iron regulatory pathway more relevant to sessile growth. This study therefore
515 provides yet another potential mechanism for how the PrrF sRNAs may contribute to
516 pathogenesis. More broadly, our results highlight how iron regulatory pathways are highly
517 dynamic and subject to changing environmental conditions, which may have broad implications
518 for the heterogeneous conditions within the host.

519 Iron depletion was previously reported to enhance expression of T6SS systems in *P.*
520 *aeruginosa*, though this was presumed to be the result of ferric uptake regulator (Fur) regulation

521 due to the presence of a Fur consensus site in promoter of the HSI-II locus (54). In the current
522 study, we show that iron regulation of T6SS genes occurs via the PrrF sRNAs, which
523 themselves are regulated by iron via the Fur protein. Based on these data, we propose the
524 regulatory model shown in **Figure 9**, wherein the PrrF sRNAs activate HSI-II expression by
525 promoting production of the PQS and AHQ molecules, which in turn function as co-inducers of
526 the PqsR/MvfR regulatory protein. Previous studies suggest that MvfR activates expression of
527 the HSI-II T6SS loci via another quorum sensing regulator, RhlR, which directly activates HSI-II
528 T6SS promoter activity in *P. aeruginosa* strain PAO1. These previous studies showed that AQs
529 induced HSI-II T6SS in shaking cultures grown in nutrient-rich LB medium (55), whereas we
530 found that AQs were not necessary for HSI-II T6SS expression in shaking cultures grown in a
531 nutrient depleted medium (DTSB). Notably, synthesized AQs caused robust induction of T6SS
532 expression in shaking cultures of Δ*pqsA,* but not in static cultures, while culture supernatants
533 caused slight induction of T6SS expression in the Δ*pqsA* mutant in static conditions alone (**Fig.**
534 **4A,B**), suggesting that how AQs are delivered to *P. aeruginosa* impacts their ability to promote
535 T6SS expression. PQS is known to intercalate into and initiate the formation of outer membrane
536 vesicles (OMVs), which mediate PQS transport from cell to cell; HHQ transport is still not fully
537 characterized but is instead dependent on the MexEF-OprN efflux pump (69)**.** The export of
538 these molecules has not been previously studied in sessile conditions, and our current studies
539 indicate that export of C7-PQS and C9-PQS is enhanced in sessile growth conditions (**Fig. S4**).
540 Notably, exogenous PQS levels are actually higher in sessile conditions than in static conditions
541 (**Fig. S4**). As such, additional studies will be needed to determine the mechanism by which
542 sessile growth conditions alter the export and biological activity of PrrF-regulated AQs.
543 Sessile growth also revealed changes in how iron affects the expression of pyochelin
544 and phenazine biosynthetic proteins (**Fig. 6**). Recent studies of iron regulation in shaking
545 conditions showed that iron starvation diminished phenazine biosynthesis gene expression and
546 phenazine production (12, 36), while the sessile growth conditions in the current studies showed

547 that iron depletion enhanced expression of phenazine biosynthesis proteins. This difference
548 may be related to the varying role of phenazines in shaking versus sessile growth conditions.
549 For instance, phenazines can induce auto-poisoning and extracellular DNA release, and these
550 toxic effects are enhanced by nutrient depletion during aerobic shaking growth (70). However,
551 phenazines also contribute to iron acquisition and survival due to their inherent redox-cycling
552 activity, by which they are capable of catalyzing the formation of bioavailable ferrous iron from
553 ferric iron (71, 72). This may be especially pertinent in static conditions, where iron requirements
554 for biofilm formation are shown to be enhanced (73). The inherent redox-cycling activity of
555 phenazines promotes biofilm formation by promoting the reduction of ferric iron to more
556 bioavailable ferrous iron (71-73). Similarly, our study showed that pyochelin siderophore
557 biosynthetic proteins were more strongly induced by iron depletion in static cultures (**Fig. 2**).
558 While pyochelin is primarily appreciated for its role in the acquisition of ferric iron, iron-bound
559 pyochelin can also promote the production of reactive oxygen species, particularly in
560 conjunction to phenazines (74-77). As such, coordinated production of phenazines and
561 pyochelin in sessile cultures may function to promote *P. aeruginosa* biofilm formation. Biofilms
562 are an important adaptive feature of *P. aeruginosa* infection, and the appearance of robust
563 biofilm-producing *P. aeruginosa* isolates during chronic lung infections is associated with
564 increased mortality in CF patients (4, 78, 79). While the current study did not specifically
565 address the impact of iron depletion within biofilm communities, the distinct effects of iron during
566 sessile growth may be relevant to *P. aeruginosa's* ability to form biofilms during chronic
567 infections.

568 In addition to promoting virulence in mammalian hosts, many of the iron-regulated
569 systems discussed in this report have been implicated in polymicrobial interactions. Previous
570 work from our own groups showed that iron depletion enhanced the production of AQs, thereby
571 enhancing antimicrobial activity during co-culture with *S. aureus* (23). While this earlier work
572 suggested that PrrF was not required for this regulatory effect, the current study demonstrates

573 that the role of PrrF in antimicrobial activity is dependent on culture agitation. Specifically, we
574 show that PrrF is required for antimicrobial activity in shaking cultures, but dispensable in static
575 cultures. Our work further highlighted distinct roles of different AQ species in mediating
576 antimicrobial activity in shaking versus static conditions. Notably, we observed greatly
577 diminished levels of AQNOs in sessile cultures, while AHQ levels were substantially increased.
578 Thus the mechanism of antimicrobial activity against *S. aureus* is likely quite different between
579 shaking and sessile cultures. Interestingly, Filkins *et al* previously showed that AQNOs were
580 critical for antimicrobial activity against *S. aureus* in biofilms grown on CF bronchial epithelial
581 cells (24), which might be expected to more closely mimic our static versus shaking conditions.
582 This apparent inconsistency could be due to any number of differences between the culture
583 conditions used here and in the Filkins study, including the time to form a mature biofilm, media
584 selection, and the presence of mammalian cell lines. Consistent with this previous study,
585 however, we found that siderophore-mediated iron uptake was critical for antimicrobial activity.
586 Our analyses of how T6SS impacts antimicrobial activity were unfortunately less conclusive,
587 due in part to the weak antimicrobial activity of the *P. aeruginosa* transposon mutant parent
588 strain, mPAO1. While T6SSs have been shown to deliver toxins to Gram-negative bacteria as
589 well as host cells, interspecies delivery to Gram-positive bacteria has not been demonstrated,
590 making this an intriguing direction for future studies. However, because PrrF sRNAs are not
591 required for AMA in sessile conditions, we predict that PrrF-dependent T6SS is not a key
592 mediator of polymicrobial interactions in our current assays.

593 Iron availability plays a critical role in the ability of *P. aeruginosa* to express a variety of
594 virulence traits, including the production of secondary metabolites, toxin secretion, and biofilm
595 formation. The Fur protein and PrrF sRNAs maintain tight control over the expression of many
596 of these activities in response to iron availability. However, these regulatory networks have not
597 been fully characterized in sessile communities, which are likely to more closely reflect
598 conditions in the host. The current study highlights the dramatic impact that sessile growth has

599 on key iron regulatory pathways in *P. aeruginosa*, and highlights to need to further investigate
600 iron regulation in sessile microbial communities such as biofilms. Such studies are likely to
601 reveal many more striking physiological adaptations that are critical for chronic *P. aeruginosa*
602 infections, yielding novel targets for the development of effective antimicrobial therapies.
603

604 **ACKNOWLEDGMENTS**

605 This work was funded in part by the National Institutes of Health (NIH) grants R01
606 AI123320 (to AGO), T32 GM066706 (to LKB), the Cystic Fibrosis Foundation grant
607 CFFOGLESB17G0 (to AGO), and the University of Maryland, School of Pharmacy Mass
608 Spectrometry Center (SOP1841-IQB2014). We thank members of the Oglesby laboratory for
609 editing of the manuscript, and Dr. Angela Wilks for thoughtful discussions and feedback as the
610 study progressed.
611

612 **REFERENCES**

613 1. Koch C (2002) Early infection and progression of cystic fibrosis lung disease. *Pediatr*
614 *Pulmonol* 34(3):232-236.10.1002/ppul.10135
615 2. Li Z*, et al.* (2005) Longitudinal development of mucoid Pseudomonas aeruginosa
616 infection and lung disease progression in children with cystic fibrosis. *JAMA* 293(5):581-
617 588.10.1001/jama.293.5.581
618 3. Paganin P*, et al.* (2015) Changes in cystic fibrosis airway microbial community
619 associated with a severe decline in lung function. *PLoS One*
620 10(4):e0124348.10.1371/journal.pone.0124348
621 4. Kerem E, Corey M, Gold R, & Levison H (1990) Pulmonary function and clinical course
622 in patients with cystic fibrosis after pulmonary colonization with *Pseudomonas*
623 *aeruginosa*. *J Pediatr* 116(5):714-719

624 5. Scheetz MH*, et al.* (2009) Morbidity associated with *Pseudomonas aeruginosa*
625 bloodstream infections. *Diagn Microbiol Infect Dis* 64(3):311-
626 319.10.1016/j.diagmicrobio.2009.02.006
627 6. Wisplinghoff H*, et al.* (2004) Nosocomial bloodstream infections in US hospitals: analysis
628 of 24,179 cases from a prospective nationwide surveillance study. *Clin Infect Dis*
629 39(3):309-317.10.1086/421946
630 7. CDC (2019) *Antibiotic Resistance Threats in the United States, 2019* (Atlanta, GA.),
631 U.S. Dept of Health and Human Services.
632 8. Reid DW, Withers NJ, Francis L, Wilson JW, & Kotsimbos TC (2002) Iron deficiency in
633 cystic fibrosis: relationship to lung disease severity and chronic *Pseudomonas*
634 *aeruginosa* infection. *Chest* 121(1):48-54
635 9. Reinhart AA*, et al.* (2017) The *Pseudomonas aeruginosa* PrrF small RNAs regulate iron
636 homeostasis during acute murine lung infection. *Infection and immunity*
637 85(5).10.1128/IAI.00764-16
638 10. Hood MI & Skaar EP (2012) Nutritional immunity: transition metals at the pathogen-host
639 interface. *Nat Rev Microbiol* 10(8):525-537.10.1038/nrmicro2836
640 11. Wakeman CA*, et al.* (2016) The innate immune protein calprotectin promotes
641 *Pseudomonas aeruginosa* and *Staphylococcus aureus* interaction. *Nat Commun*
642 7:11951.10.1038/ncomms11951
643 12. Zygiel EM, Nelson CE, Brewer LK, Oglesby-Sherrouse AG, & Nolan EM (2019) The
644 human innate immune protein calprotectin induces iron starvation responses in
645 Pseudomonas aeruginosa. *J Biol Chem* 294(10):3549-3562.10.1074/jbc.RA118.006819
646 13. Kim EJ, Sabra W, & Zeng AP (2003) Iron deficiency leads to inhibition of oxygen transfer
647 and enhanced formation of virulence factors in cultures of *Pseudomonas aeruginosa*
648 PAO1. *Microbiology* 149(Pt 9):2627-2634.10.1099/mic.0.26276-0

649 14. Vasil ML & Ochsner UA (1999) The response of *Pseudomonas aeruginosa* to iron:
650 genetics, biochemistry and virulence. *Molecular microbiology* 34(3):399-413
651 15. Wiens JR, Vasil AI, Schurr MJ, & Vasil ML (2014) Iron-regulated expression of alginate
652 production, mucoid phenotype, and biofilm formation by *Pseudomonas aeruginosa*.
653 *MBio* 5(1):e01010-01013.10.1128/mBio.01010-13
654 16. Oglesby AG*, et al.* (2008) The influence of iron on *Pseudomonas aeruginosa* physiology:
655 a regulatory link between iron and quorum sensing. *J Biol Chem* 283(23):15558-
656 15567.10.1074/jbc.M707840200
657 17. Torres VJ*, et al.* (2010) *Staphylococcus aureus fur* regulates the expression of virulence
658 factors that contribute to the pathogenesis of pneumonia. *Infection and immunity*
659 78(4):1618-1628.10.1128/IAI.01423-09
660 18. Friedman DB*, et al.* (2006) *Staphylococcus aureus* redirects central metabolism to
661 increase iron availability. *PLoS pathogens* 2(8):e87.10.1371/journal.ppat.0020087
662 19. Ochsner UA & Vasil ML (1996) Gene repression by the ferric uptake regulator in
663 *Pseudomonas aeruginosa*: cycle selection of iron-regulated genes. *Proceedings of the*
664 *National Academy of Sciences of the United States of America* 93(9):4409-4414
665 20. Nguyen AT*, et al.* (2016) Cystic Fibrosis Isolates of *Pseudomonas aeruginosa* Retain
666 Iron-Regulated Antimicrobial Activity against *Staphylococcus aureus* through the Action
667 of Multiple Alkylquinolones. *Front Microbiol* 7:1171.10.3389/fmicb.2016.01171
668 21. Reinhart AA*, et al.* (2015) The prrF-encoded small regulatory RNAs are required for iron
669 homeostasis and virulence of Pseudomonas aeruginosa. *Infect Immun* 83(3):863-
670 875.10.1128/IAI.02707-14
671 22. Mashburn LM, Jett AM, Akins DR, & Whiteley M (2005) *Staphylococcus aureus* serves
672 as an iron source for *Pseudomonas aeruginosa* during *in vivo* coculture. *Journal of*
673 *bacteriology* 187(2):554-566

674 23. Nguyen AT, Jones JW, Ruge MA, Kane MA, & Oglesby-Sherrouse AG (2015) Iron
675 Depletion Enhances Production of Antimicrobials by *Pseudomonas aeruginosa*. *J*
676 *Bacteriol* 197(14):2265-2275.10.1128/JB.00072-15
677 24. Filkins LM*, et al.* (2015) Coculture of *Staphylococcus aureus* with *Pseudomonas*
678 *aeruginosa* Drives *S. aureus* towards Fermentative Metabolism and Reduced Viability in
679 a Cystic Fibrosis Model. *J Bacteriol* 197(14):2252-2264.10.1128/JB.00059-15
680 25. Szamosvari D & Bottcher T (2017) An Unsaturated Quinolone N-Oxide of *Pseudomonas*
681 *aeruginosa* Modulates Growth and Virulence of *Staphylococcus aureus*. *Angew Chem*
682 *Int Ed Engl* 56(25):7271-7275.10.1002/anie.201702944
683 26. Lightbown JW & Jackson FL (1956) Inhibition of cytochrome systems of heart muscle
684 and certain bacteria by the antagonists of dihydrostreptomycin: 2-alkyl-4-
685 hydroxyquinoline N-oxides. *Biochem J* 63(1):130-137
686 27. Reil E, Hofle G, Draber W, & Oettmeier W (1997) Quinolones and their N-oxides as
687 inhibitors of mitochondrial complexes I and III. *Biochim Biophys Acta* 1318(1-2):291-
688 298.10.1016/s0005-2728(96)00150-8
689 28. Collier DN*, et al.* (2002) A bacterial cell to cell signal in the lungs of cystic fibrosis
690 patients. *FEMS Microbiol Lett* 215(1):41-46
691 29. Bredenbruch F, Geffers R, Nimtz M, Buer J, & Haussler S (2006) The *Pseudomonas*
692 *aeruginosa* quinolone signal (PQS) has an iron-chelating activity. *Environ Microbiol*
693 8(8):1318-1329.10.1111/j.1462-2920.2006.01025.x
694 30. Pesci EC*, et al.* (1999) Quinolone signaling in the cell-to-cell communication system of
695 *Pseudomonas aeruginosa*. *Proc Natl Acad Sci U S A* 96(20):11229-11234
696 31. Florez C, Raab JE, Cooke AC, & Schertzer JW (2017) Membrane Distribution of the
697 Pseudomonas Quinolone Signal Modulates Outer Membrane Vesicle Production in
698 *Pseudomonas aeruginosa*. *MBio* 8(4).10.1128/mBio.01034-17

699 32. Coleman JP*, et al.* (2008) *Pseudomonas aeruginosa* PqsA is an anthranilate-coenzyme
700 A ligase. *Journal of bacteriology* 190(4):1247-1255.10.1128/JB.01140-07
701 33. Djapgne L*, et al.* (2018) The *Pseudomonas aeruginosa* PrrF1 and PrrF2 small regulatory
702 RNAs (sRNAs) promote 2-alkyl-4-quinolone production through redundant regulation of
703 the antR mRNA. *J Bacteriol*.10.1128/JB.00704-17
704 34. Beauchene NA*, et al.* (2015) Impact of Anaerobiosis on Expression of the Iron-
705 Responsive Fur and RyhB Regulons. *mBio* 6(6):e01947-01915.10.1128/mBio.01947-15
706 35. Sampathkumar B*, et al.* (2006) Transcriptional and translational expression patterns
707 associated with immobilized growth of Campylobacter jejuni. *Microbiology* 152(Pt 2):567-
708 577.10.1099/mic.0.28405-0
709 36. Nelson CE*, et al.* (2019) Proteomic analysis of the *Pseudomonas aeruginosa* iron
710 starvation response reveals PrrF sRNA-dependent iron regulation of twitching motility,
711 amino acid metabolism, and zinc homeostasis proteins. *J Bacteriol*.10.1128/JB.00754-
712 18
713 37. Erde J, Loo RR, & Loo JA (2014) Enhanced FASP (eFASP) to increase proteome
714 coverage and sample recovery for quantitative proteomic experiments. *J Proteome Res*
715 13(4):1885-1895.10.1021/pr4010019
716 38. Wisniewski JR, Zougman A, Nagaraj N, & Mann M (2009) Universal sample preparation
717 method for proteome analysis. *Nat Methods* 6(5):359-362.10.1038/nmeth.1322
718 39. Winsor GL*, et al.* (2016) Enhanced annotations and features for comparing thousands of
719 Pseudomonas genomes in the Pseudomonas genome database. *Nucleic Acids Res*
720 44(D1):D646-653.10.1093/nar/gkv1227
721 40. Eng JK, Fischer B, Grossmann J, & Maccoss MJ (2008) A fast SEQUEST cross
722 correlation algorithm. *J Proteome Res* 7(10):4598-4602.10.1021/pr800420s
723 41. Dorfer V*, et al.* (2014) MS Amanda, a universal identification algorithm optimized for high
724 accuracy tandem mass spectra. *J Proteome Res* 13(8):3679-3684.10.1021/pr500202e

725 42. Kall L, Canterbury JD, Weston J, Noble WS, & MacCoss MJ (2007) Semi-supervised
726 learning for peptide identification from shotgun proteomics datasets. *Nat Methods*
727 4(11):923-925.10.1038/nmeth1113
728 43. Kanehisa M, Sato Y, Kawashima M, Furumichi M, & Tanabe M (2016) KEGG as a
729 reference resource for gene and protein annotation. *Nucleic Acids Res* 44(D1):D457-
730 462.10.1093/nar/gkv1070
731 44. Huang W*, et al.* (2018) PAMDB: a comprehensive Pseudomonas aeruginosa
732 metabolome database. *Nucleic Acids Res* 46(D1):D575-D580.10.1093/nar/gkx1061
733 45. Szklarczyk D*, et al.* (2017) The STRING database in 2017: quality-controlled protein-
734 protein association networks, made broadly accessible. *Nucleic Acids Res* 45(D1):D362-
735 D368.10.1093/nar/gkw937
736 46. Brewer LK*, et al.* (2019) Development and Bioanalytical Method Validation of an LC-
737 MS/MS Assay for Simultaneous Quantitation of 2-Alkyl-4(1H)-Quinolones for Application
738 in Bacterial Cell Culture and Lung Tissue. *Submitted*
739 47. Ochsner UA, Wilderman PJ, Vasil AI, & Vasil ML (2002) GeneChip expression analysis
740 of the iron starvation response in *Pseudomonas aeruginosa*: identification of novel
741 pyoverdine biosynthesis genes. *Mol Microbiol* 45(5):1277-1287.10.1046/j.1365-
742 2958.2002.03084.x
743 48. Poole K, Heinrichs DE, & Neshat S (1993) Cloning and sequence analysis of an EnvCD
744 homologue in *Pseudomonas aeruginosa*: regulation by iron and possible involvement in
745 the secretion of the siderophore pyoverdine. *Molecular microbiology* 10(3):529-544
746 49. Ankenbauer RG & Quan HN (1994) FptA, the Fe(III)-pyochelin receptor of
747 *Pseudomonas aeruginosa*: a phenolate siderophore receptor homologous to
748 hydroxamate siderophore receptors. *J Bacteriol* 176(2):307-319

749 50. Dean CR & Poole K (1993) *Cloning and characterizati*on of the ferric enterobactin
750 receptor gene (pfeA) of Pseudomonas aeruginosa. *Journal of bacteriology* 175(2):317-
751 324
752 51. Serino L*, et al.* (1997) Biosynthesis of pyochelin and dihydroaeruginoic acid requires the
753 iron-regulated pchDCBA operon in *Pseudomonas aeruginosa*. *J Bacteriol* 179(1):248-
754 257
755 52. Hassett DJ*, et al.* (1997) An operon containing fumC and sodA encoding fumarase C
756 and manganese superoxide dismutase is controlled by the ferric uptake regulator in
757 *Pseudomonas aeruginosa*: fur mutants produce elevated alginate levels. *J Bacteriol*
758 179(5):1452-1459
759 53. Wilderman PJ*, et al.* (2004) Identification of tandem duplicate regulatory small RNAs in
760 *Pseudomonas aeruginosa* involved in iron homeostasis. *Proceedings of the National*
761 *Academy of Sciences of the United States of America* 101(26):9792-
762 9797.10.1073/pnas.0403423101
763 54. Sana TG*, et al.* (2012) The second type VI secretion system of *Pseudomonas*
764 *aeruginosa* strain PAO1 is regulated by quorum sensing and Fur and modulates
765 internalization in epithelial cells. *J Biol Chem* 287(32):27095-
766 27105.10.1074/jbc.M112.376368
767 55. Lesic B, Starkey M, He J, Hazan R, & Rahme LG (2009) Quorum sensing differentially
768 regulates *Pseudomonas aeruginosa* type VI secretion locus I and homologous loci II and
769 III, which are required for pathogenesis. *Microbiology* 155(Pt 9):2845-
770 2855.10.1099/mic.0.029082-0
771 56. Gaines JM, Carty NL, Colmer-Hamood JA, & Hamood AN (2005) Effect of static growth
772 and different levels of environmental oxygen on toxA and ptxR expression in the
773 *Pseudomonas aeruginosa* strain PAO1. *Microbiology* 151(Pt 7):2263-
774 2275.10.1099/mic.0.27754-0

775 57. Wyckoff TJ, Thomas B, Hassett DJ, & Wozniak DJ (2002) Static growth of mucoid
776 *Pseudomonas aeruginosa* selects for non-mucoid variants that have acquired flagellum-
777 dependent motility. *Microbiology* 148(Pt 11):3423-3430.10.1099/00221287-148-11-3423
778 58. Dotsch A*, et al.* (2012) The *Pseudomonas aeruginosa* transcriptome in planktonic
779 cultures and static biofilms using RNA sequencing. *PLoS One*
780 7(2):e31092.10.1371/journal.pone.0031092
781 59. Schertzer JW, Brown SA, & Whiteley M (2010) Oxygen levels rapidly modulate
782 *Pseudomonas aeruginosa* social behaviours via substrate limitation of PqsH. *Mol*
783 *Microbiol* 77(6):1527-1538.10.1111/j.1365-2958.2010.07303.x
784 60. Drees SL*, et al.* (2018) PqsL uses reduced flavin to produce 2-
785 hydroxylaminobenzoylacetate, a preferred PqsBC substrate in alkyl quinolone
786 biosynthesis in *Pseudomonas aeruginosa*. *J Biol Chem* 293(24):9345-
787 9357.10.1074/jbc.RA117.000789
788 61. Jacobs MA*, et al.* (2003) Comprehensive transposon mutant library of *Pseudomonas*
789 *aeruginosa*. *Proc Natl Acad Sci U S A* 100(24):14339-14344.10.1073/pnas.2036282100
790 62. Brint JM & Ohman DE (1995) Synthesis of multiple exoproducts in Pseudomonas
791 aeruginosa is under the control of RhlR-RhlI, another set of regulators in strain PAO1
792 with homology to the autoinducer-responsive LuxR-LuxI family. *J Bacteriol*
793 177(24):7155-7163.10.1128/jb.177.24.7155-7163.1995
794 63. Ochsner UA & Reiser J (1995) Autoinducer-mediated regulation of rhamnolipid
795 biosurfactant synthesis in Pseudomonas aeruginosa. *Proc Natl Acad Sci U S A*
796 92(14):6424-6428.10.1073/pnas.92.14.6424
797 64. Deziel E*, et al.* (2005) The contribution of MvfR to Pseudomonas aeruginosa
798 pathogenesis and quorum sensing circuitry regulation: multiple quorum sensing-
799 regulated genes are modulated without affecting lasRI, rhlRI or the production of N-acyl-

800 L-homoserine lactones. *Mol Microbiol* 55(4):998-1014.10.1111/j.1365-
801 2958.2004.04448.x
802 65. Xiao G*, et al.* (2006) MvfR, a key Pseudomonas aeruginosa pathogenicity LTTR-class
803 regulatory protein, has dual ligands. *Mol Microbiol* 62(6):1689-1699.10.1111/j.1365-
804 2958.2006.05462.x
805 66. Gallagher LA, McKnight SL, Kuznetsova MS, Pesci EC, & Manoil C (2002) Functions
806 required for extracellular quinolone signaling by Pseudomonas aeruginosa. *J Bacteriol*
807 184(23):6472-6480
808 67. Russell AB*, et al.* (2013) Diverse type VI secretion phospholipases are functionally
809 plastic antibacterial effectors. *Nature* 496(7446):508-512.10.1038/nature12074
810 68. Hood RD*, et al.* (2010) A type VI secretion system of *Pseudomonas aeruginosa* targets
811 a toxin to bacteria. *Cell Host Microbe* 7(1):25-37.10.1016/j.chom.2009.12.007
812 69. Lamarche MG & Deziel E (2011) MexEF-OprN efflux pump exports the Pseudomonas
813 quinolone signal (PQS) precursor HHQ (4-hydroxy-2-heptylquinoline). *PLoS One*
814 6(9):e24310.10.1371/journal.pone.0024310
815 70. Meirelles LA & Newman DK (2018) Both toxic and beneficial effects of pyocyanin
816 contribute to the lifecycle of *Pseudomonas aeruginosa*. *Mol Microbiol* 110(6):995-
817 1010.10.1111/mmi.14132
818 71. Glasser NR, Kern SE, & Newman DK (2014) Phenazine redox cycling enhances
819 anaerobic survival in *Pseudomonas aeruginosa* by facilitating generation of ATP and a
820 proton-motive force. *Mol Microbiol* 92(2):399-412.10.1111/mmi.12566
821 72. Wang Y*, et al.* (2011) Phenazine-1-carboxylic acid promotes bacterial biofilm
822 development via ferrous iron acquisition. *J Bacteriol* 193(14):3606-
823 3617.10.1128/JB.00396-11

824 73. O'May CY, Sanderson K, Roddam LF, Kirov SM, & Reid DW (2009) Iron-binding
825 compounds impair *Pseudomonas aeruginosa* biofilm formation, especially under
826 anaerobic conditions. *J Med Microbiol* 58(Pt 6):765-773.10.1099/jmm.0.004416-0
827 74. Wang Y & Newman DK (2008) Redox reactions of phenazine antibiotics with ferric
828 (hydr)oxides and molecular oxygen. *Environ Sci Technol* 42(7):2380-
829 2386.10.1021/es702290a
830 75. Britigan BE*, et al.* (1992) Interaction of the *Pseudomonas aeruginosa* secretory products
831 pyocyanin and pyochelin generates hydroxyl radical and causes synergistic damage to
832 endothelial cells. Implications for *Pseudomonas*-associated tissue injury. *J Clin Invest*
833 90(6):2187-2196.10.1172/JCI116104
834 76. Britigan BE, Rasmussen GT, & Cox CD (1997) Augmentation of oxidant injury to human
835 pulmonary epithelial cells by the *Pseudomonas aeruginosa* siderophore pyochelin. *Infect*
836 *Immun* 65(3):1071-1076
837 77. Coffman TJ, Cox CD, Edeker BL, & Britigan BE (1990) Possible role of bacterial
838 siderophores in inflammation. Iron bound to the *Pseudomonas* siderophore pyochelin
839 can function as a hydroxyl radical catalyst. *J Clin Invest* 86(4):1030-
840 1037.10.1172/JCI114805
841 78. Henry RL, Mellis CM, & Petrovic L (1992) Mucoid *Pseudomonas aeruginosa* is a marker
842 of poor survival in cystic fibrosis. *Pediatr Pulmonol* 12(3):158-161
843 79. Pedersen SS, Hoiby N, Espersen F, & Koch C (1992) Role of alginate in infection with
844 mucoid *Pseudomonas aeruginosa* in cystic fibrosis. *Thorax* 47(1):6-13
845

FIGURES AND FIGURE LEGENDS

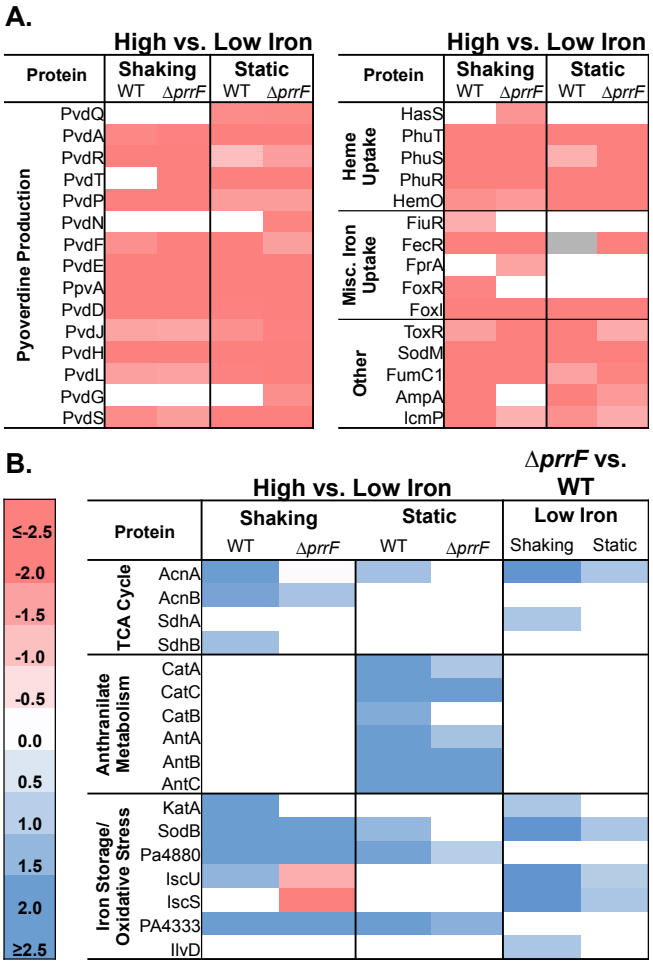

Figure 1. Static growth reduces the effects of classical PrrF regulation. Heatmaps showing the $\log_2$ fold change (LFC) of **(A)** known iron-repressed proteins and **(B)** known PrrF-regulated proteins, in the indicated strains grown in high versus low iron conditions or in the Δ*prrF* mutant versus wild type PAO1 grown in low iron conditions. Wild type PAO1 and Δ*prrF* strains were inoculated into 1.5mL DTSB supplemented with either iron (0μM) or high iron (100μM) and incubated in shaking or static conditions. LC-MS/MS-based proteomics analysis showed statistically significant protein regulation (FDR adjusted p-value < 0.05) of known iron and PrrF targets, as indicated by at least 2-fold induction or repression (i.e. 1 LFC) in response to treatment. Gray boxes indicate proteins that were undetected in one or more condition. White boxes indicate no significant change in gene expression was observed.

858

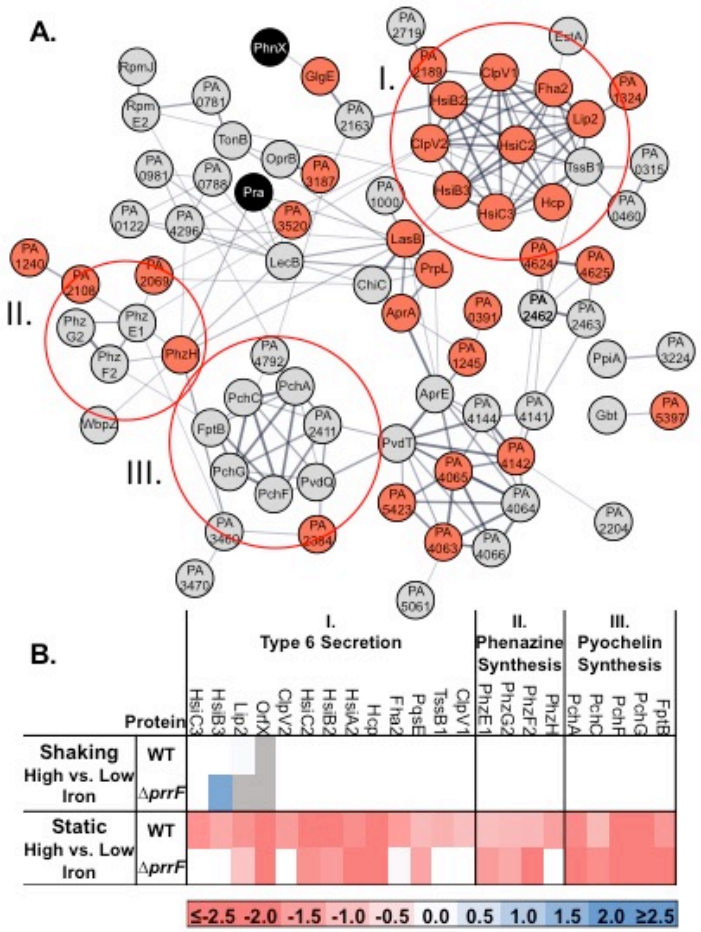

859

860 **Figure 2. Proteomics reveals novel targets of iron regulation in static conditions.** Wild
861 type PAO1 and the Δ*prrF* strain were inoculated into 1.5mL DTSB media and supplemented
862 with either low iron (0μM) or high iron (100μM) and incubated in either shaking or static
863 conditions. Statistically significant iron regulation (FDR adjusted p-value < 0.05) in static and
864 shaking conditions was identified by at least 2-fold (i.e.1 LFC) induction in response to iron
865 starvation as described in Materials and Methods. **(A)** Network analysis of differentially
866 regulated genes was carried out using STRING database software, which revealed distinct
867 several virulence-associated genes that were similarly impacted by iron starvation under static
868 conditions. Line thickness indicates strength of data support for association between two
869 proteins, as calculated by STRING network analysis (45). Red nodes represent genes which

870 were significantly regulated by PrrF in low iron static conditions, gray nodes indicated genes that
871 do not exhibit regulation by PrrF. Black nodes represent genes that exhibited iron regulation in
872 static conditions but were not detected in one or more iron conditions in shaking cultures. **(B)**
873 Heatmaps of differentially regulated genes from HSI-II T6SS, phenazine, and pyochelin
874 biosynthetic operons. Gray boxes indicate proteins that were not detected in one or more
875 condition. White boxes indicate that no significant change in gene expression was observed.
876

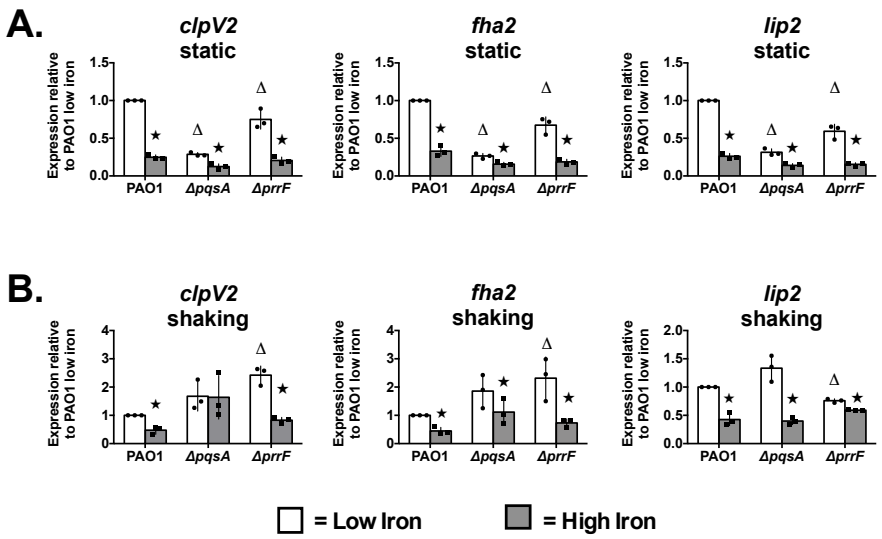

877

878 **Figure 3. AQs differentially regulate expression of T6SS genes in sessile and shaking**

879 **conditions.** Cultures were grown in 1.5 mL of DTSB media supplemented with either 0μM

880 $FeCl_3$ or 100μM $FeCl_3$ in 14mL polystyrene round bottom culture tubes for 18 hours at 37˚C.

881 Cultures were incubated **(A)** without perturbation (0rpm) or (**B**) with perturbation (250rpm) prior

882 to RNA extraction (**Methods and Materials)**. Bars in each graph indicate the average value of 3

883 independent experiments (error bars represent standard deviation), and individual data points

884 from biological replicates are indicated by black circles. Asterisks represent a significant

885 difference relative to low iron PAO1, whereas triangles indicate a significant difference in

886 expression relative to low iron within a strain, as determined by a two-tailed Student's *t* test as

887 follows: *p<0.05; **p<0.005; ***p<0.0005.

888

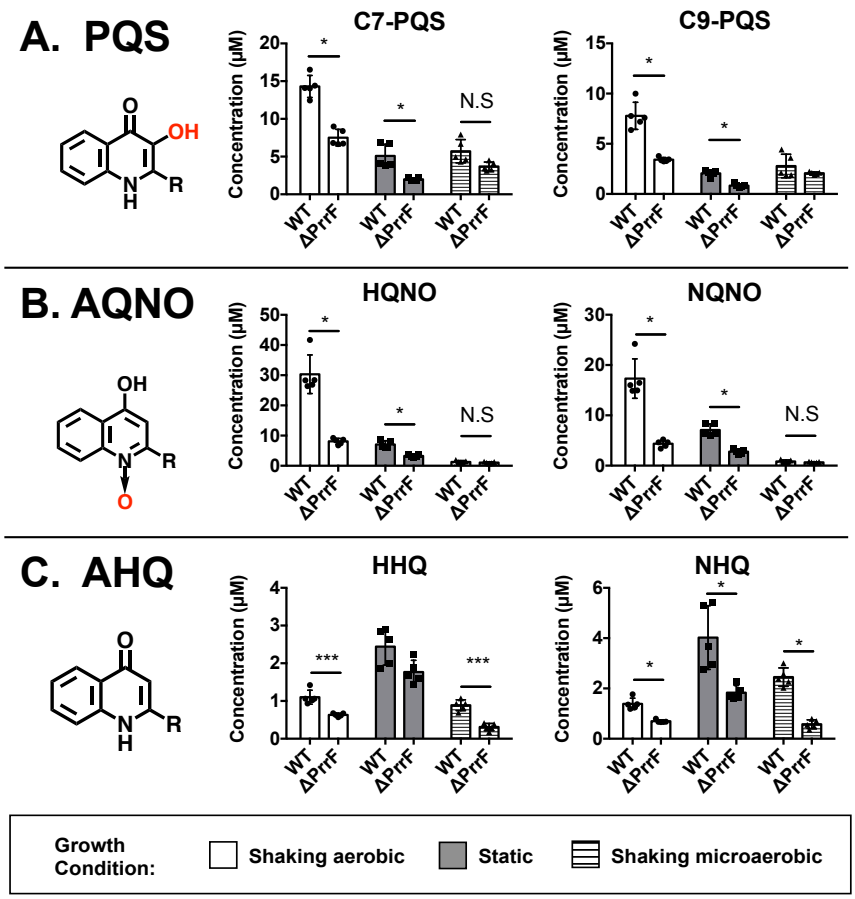

Figure 4. Concentrations of AQs in shaking, static, and microaerobic cultures of *P. aeruginosa.* Cultures were grown in 1.5 mL of iron-deplete DTSB media in 14mL polystyrene round bottom culture tubes and incubated for 18 hours at 37˚C. Microaerobic cultures were sealed in an air-tight GasPak™ system in the presence of an EZ Campy Container™ packet. Shaking and microaerobic cultures were incubated with perturbation (250rpm). Sessile cultures were incubated in shaking incubators with no perturbation (0rpm). Representative structures for (**A**) PQS molecules, (**B**) AQNO molecules, and (**C**) AHQ molecules are depicted in black, with oxygen-dependent structural elements highlighted in red (R indicates alkyl chain). AQs were quantified by LC-MS/MS where bars in each graph indicate the average concentration of 5 independent experiments and individual data points from biological replicates are indicated by black circles (error bars represent standard deviation). Asterisks indicate a significant difference as determined by a two-tailed Student's *t* test as follows: *p<0.05; **p<0.005; ***p<0.0005.

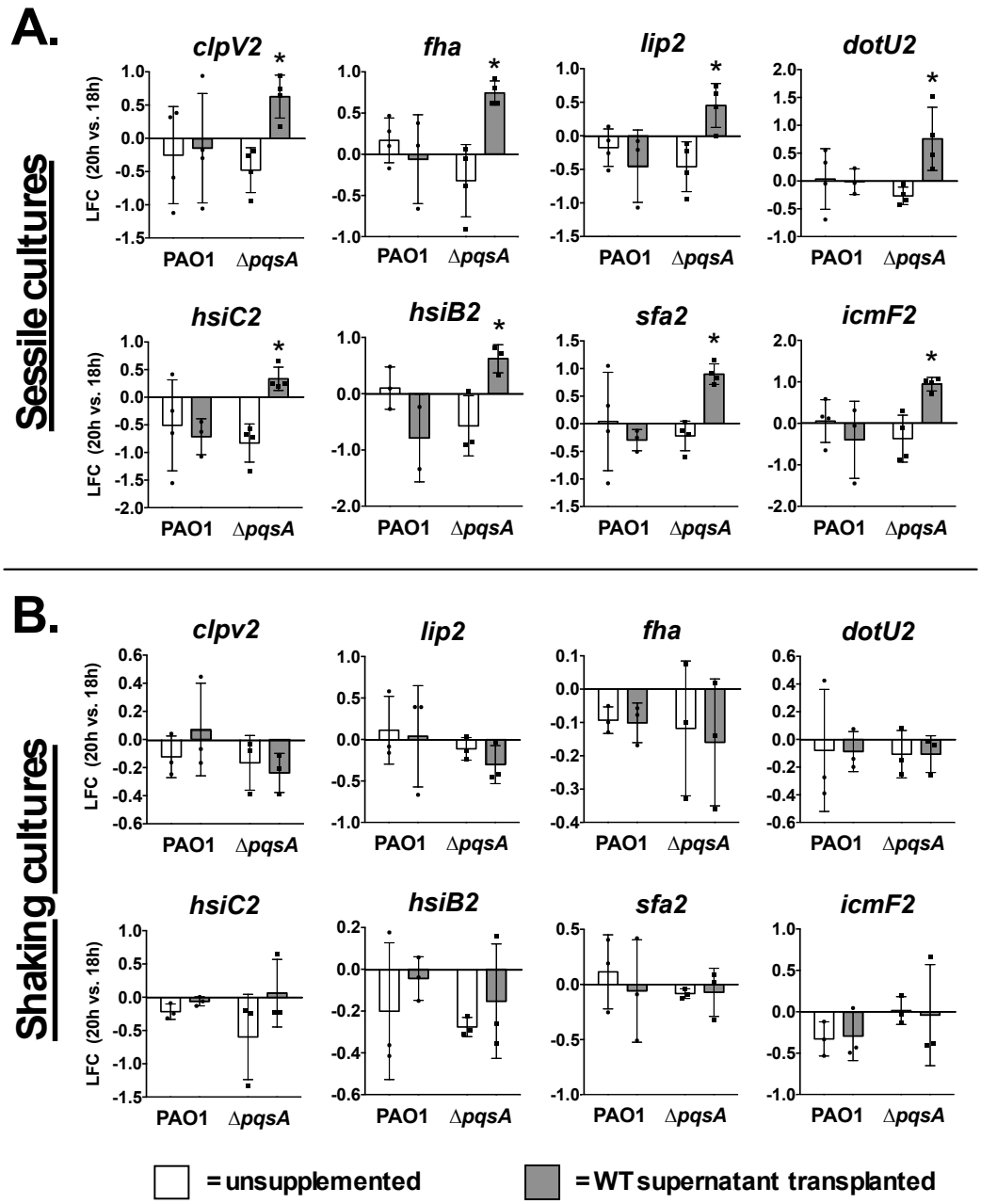

Figure 5. Supernatant transplants from WT induces expression of T6SS genes in Δ*pqsA* strain. Wild type and Δ*pqsA* cultures were grown in 1.5 mL of DTSB media supplemented with either 0μM $FeCl_3$ or 100μM $FeCl_3$ in 14mL polystyrene round bottom culture tubes for 18 hours at 37˚C. Cultures were incubated **(A)** without perturbation (0rpm) or (**B**) with perturbation (250rpm) prior to RNA extraction (**Methods and Materials)**. Cells receiving supernatant

908 transplants were centrifuged, their supernatant was removed, and then resuspended in an
909 equivalent volume of centrifuged supernatant from wild type PAO1. Cultures were grown for an
910 additional 2 hours, and subjected to qRT-PCR analysis to determine the LFC in gene
911 expression from within each strain from 18h to 20h. Bars in each graph indicate the average
912 value of 3 independent experiments (error bars represent standard deviation), and individual
913 data points from biological replicates are indicated by black circles. Asterisks represent a
914 significant difference relative to un-supplemented controls, as determined by a two-tailed
915 Student's *t* test with a significance threshold of $p \leq 0.05$.
916

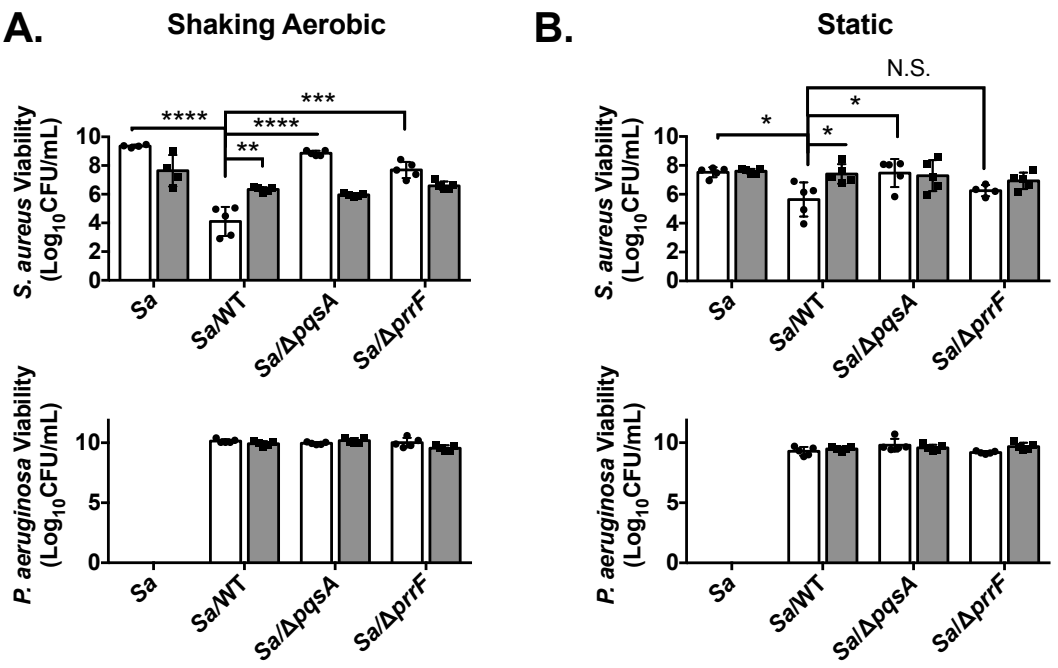

Figure 6. PrrF-mediated antimicrobial activity is altered in shaking conditions. *P. aeruginosa* and *S. aureus* were co-inoculated in DTSB media supplemented with (high iron) or without (low iron) 100μM $FeCl_3$. Co-cultures were incubated either in 14mL round bottom polystyrene cell culture tubes in shaking aerobic conditions **(A)** or in 6 well polystyrene cell culture plates in static conditions **(B)** for 18 hours. After incubation, CFUs were enumerated as described in the Materials and Methods. Bars in each graph indicate the average value in low (white bars) or high (gray bars) iron conditions, and individual data points from biological replicates are indicated by circles (low iron) or squares (high iron). Error bars indicate the standard deviation of 5 independent experiments. Asterisks indicate a significant difference as determined by a two-tailed Student's *t* test as follows: *p≤0.05; **p≤0.005; ***p≤0.0005; ****p≤0.00005.

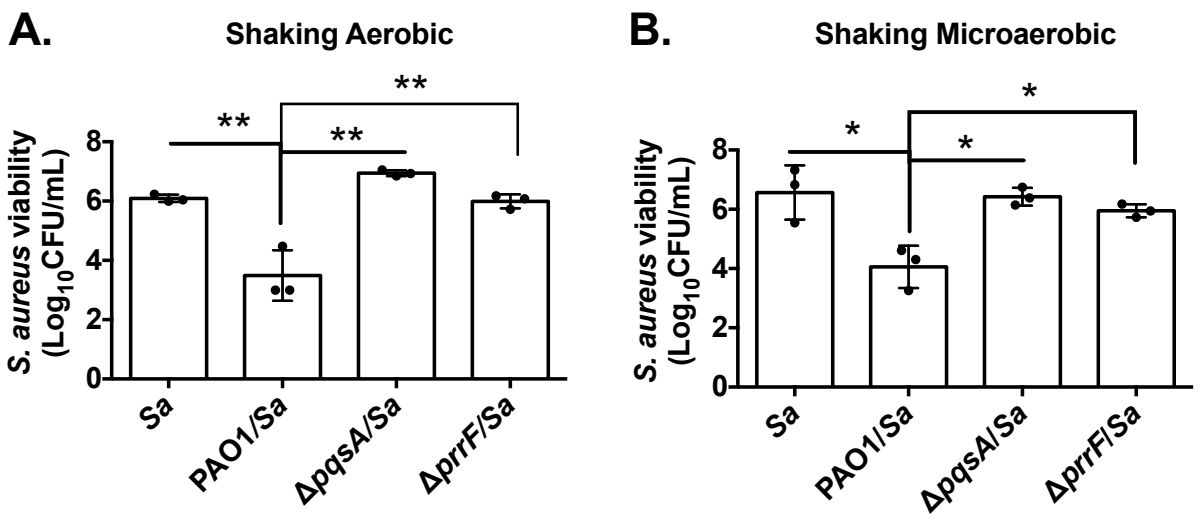

930

931 **Figure 7. *P. aeruginosa* antimicrobial activity requirement for PrrF is not influenced by**
932 **oxygen availability in co-culture with *S. aureus.*** *P. aeruginosa* and *S. aureus* were co-
933 inoculated into 1.5 mL of iron-deplete DTSB media in 14mL round-bottom polystyrene culture
934 tubes. Cultures were incubated for 18hr at 37˚C in either **(A)** shaking aerobic or in **(B)** shaking
935 microaerobic conditions. Microaerobic cultures were incubated in air-tight GasPak systems™ in
936 the presence of a GasPak EZ Campy Container™ packet to ensure microaerobic conditions.
937 After 18hr incubation, CFUs were enumerated as described above. Bars in each graph indicate
938 the average value, and individual data points from biological replicates are indicated with circles.
939 Error bars indicate the standard deviation of 5 independent experiments. Asterisks indicate a
940 significant difference as determined by a two-tailed Student's *t* test as follows: *p≤0.05;
941 **p≤0.005.

942

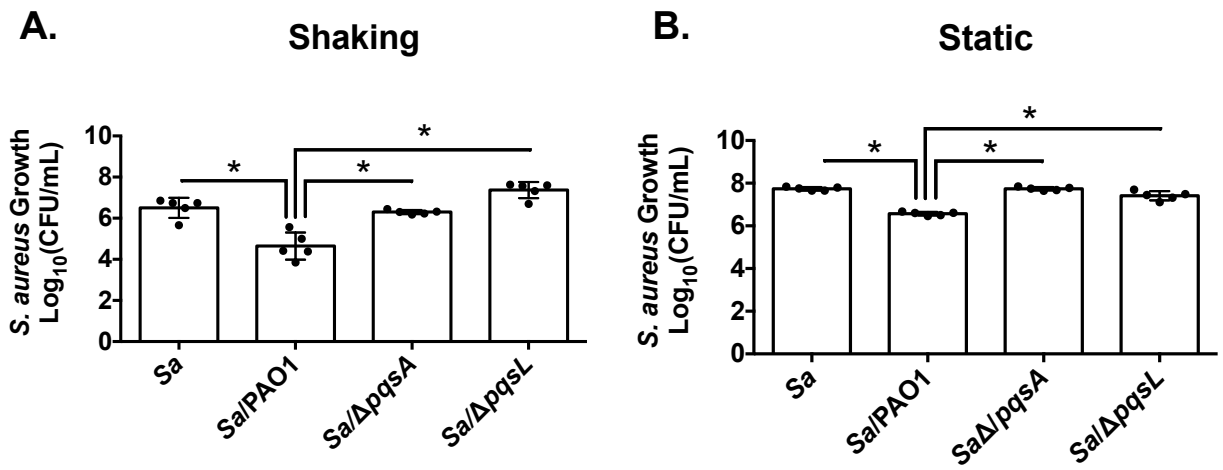

943
944 **Figure 8. AQNOs are not required for antimicrobial activity in static conditions.** *P.*
945 *aeruginosa* and *S. aureus* were co-inoculated in DTSB media supplemented with (high iron) or
946 without (low iron) 100μM $FeCl_3$. Co-cultures were incubated either in 14mL round bottom
947 polystyrene cell culture tubes in shaking aerobic conditions **(A)** or in 6 well polystyrene cell
948 culture plates in static conditions **(B)** for 18 hours. After incubation, CFUs were enumerated as
949 described in the **Materials and Methods**. Bars in each graph indicate the average value, and
950 individual data points from biological replicates are indicated by circles. Error bars indicate the
951 standard deviation of 5 independent experiments. Asterisks indicate a significant difference as
952 determined by a two-tailed Student's *t* test with a significance threshold of *$p \leq 0.05$.
953
954

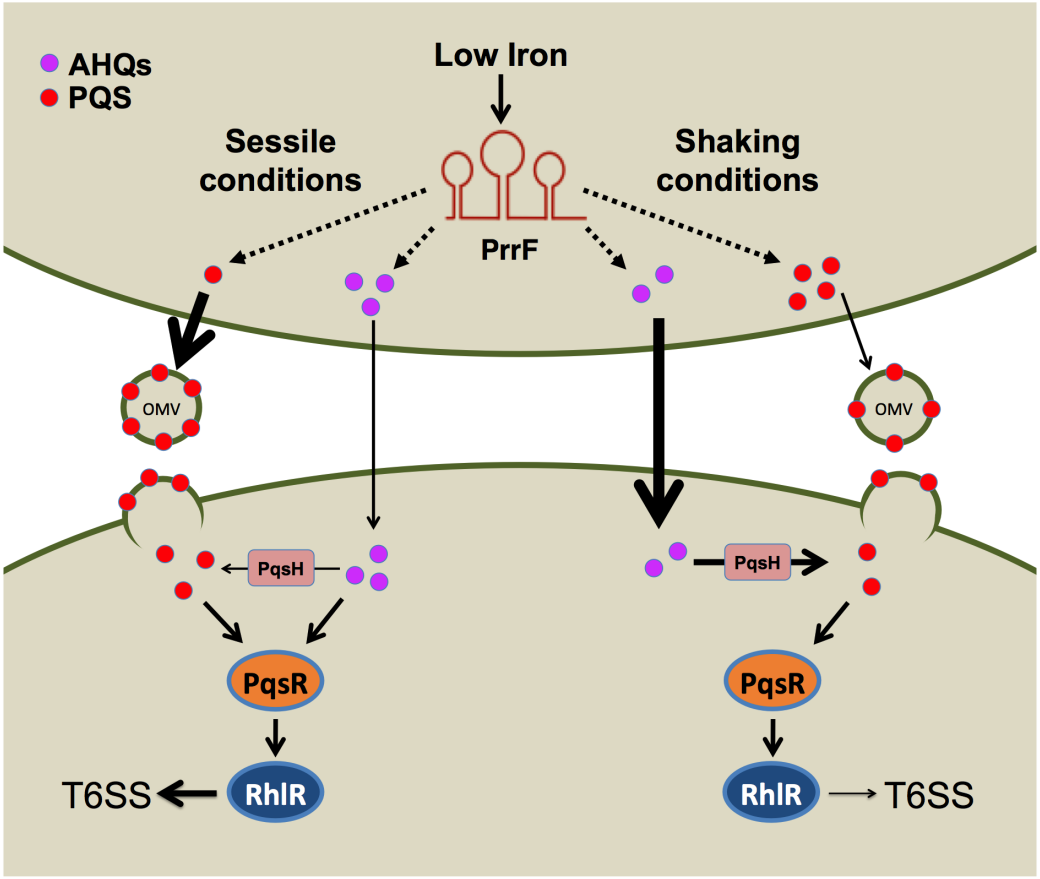

Figure 9. Proposed mechanism of PrrF-mediated iron regulation of T6SS. In both sessile and shaking conditions, low iron promotes AQ production via the PrrF sRNAs. In sessile conditions, oxygen limitation limits production of PQS molecules (red), resulting in an accumulation of the PQS precursor molecules, AHQs (purple). PQS export appears to be enhanced in sessile conditions relative to shaking conditions, and this metabolite is expected to be transported to neighboring cells via intercalation into outer membrane vesicles. In contrast, AHQ export is more efficient in shaking conditions, although the mechanism of AHQ efflux and inter-cell delivery has not been fully characterized. AHQ can be converted to PQS in both shaking and sessile conditions, but this conversion occurs more readily in shaking conditions. Once in the cell, PQS and AHQ act as cofactors for the virulence factor regulator, PqsR. PqsR in turn induces the RhlR quorum sensing system, which is a known inducer of HSI-II T6SS expression.